arXiv:cond-mat/9803275v1 [cond-mat.str-el] 23 Mar 1998

Multi-Exciton Spectroscopy of a Single Self Assembled Quantum Dot

E. Dekel[a], D. Gershoni[a], E. Ehrenfreund[a], D. Spektor[a] J.M. Garcia[b] and P.M. Petroff [b]

[a]Physics Department and Solid State Institute, Technion-Israel Institute of Technology, Haifa, Israel

[b]Materials Department, University of California, Santa Barbara, CA 93106

February 1, 2008

Abstract

We apply low temperature confocal optical microscopy to spatially resolve, and spectroscopically study a **single** self assembled quantum dot. By comparing the emission spectra obtained at various excitation levels to a theoretical many body model, we show that: Single exciton radiative recombination is very weak. Sharp spectral lines are due to optical transitions between confined multiexcitonic states among which excitons thermalize within their lifetime. Once these few states are fully occupied, broad bands appear due to transitions between states which contain continuum electrons.

The study of electronic processes in semiconductor heterostructures of reduced dimensionality has been a subject of recent extensive research efforts. Of particular importance are the efforts to fabricate and study semiconductor quantum dots (QDs) of nanometer size, in which the charge carriers are confined in all directions to characteristic lengths which are smaller than their De-Broglie wavelengths [1–16]. These efforts are motivated by both the QDs potential device applications, as well as their being an excellent stage for experimental studies of basic quantum mechanical principles. One very promising system of such QDs is called self assembled QDs (SAQDs). In fabricating SAQDs, minimization of the lattice mismatch strain between different epitaxially grown semiconductor layers occurs via the formation of small islands connected by a very thin wetting layer. By capping these self assembled islands with an epitaxial layer of wider bandgap material, with similar lattice constant to that of the substrate, high quality QDs are produced [4, 5]. This natural way of producing large ensembles of QDs has motivated a vast number of studies of their structural, electronic and optical properties [3-5,10-16]. The size distribution of these SAQDs (typically about 10%), and the resultant inhomogeneous broadening of the SAQDs characteristic features, has so far limited the ability to clearly understand and unambiguously interpret the experimental results. In this Letter, we overcome this obstacle by spectroscopically studying multi-excitonic optical transitions in a **single** SAQD. We show here, indeed, that multiple sharp spectral lines, as well as broad spectral features, which previously were interpreted as an optical signature for emission from an ensemble of dots [4, 5], are actually due to optical transitions between multi carrier states within a single dot, under various excitation levels.

The SAQD sample studied here was fabricated by deposition of a coherently strained epitaxial layer of $InAs$ on an $AlGaAs$ layer deposited on $GaAs$ substrate. The layer sequence, compositions and widths are given in the left inset to Fig. 1. During the growth of the strained layer, the sample was not rotated, thus a gradient in the QDs density was formed across its surface [10]. In particular, low density areas, in which the average distance between neighboring QDs is larger than our spatial resolution could easily be found on the sample surface. The right side inset to Fig. 1 displays the far-field ensemble photoluminescence (PL) spectrum of such an area of the SAQD sample.

We use a $\times 100$ in-situ microscope objective for diffraction limited low temperature confocal optical spectroscopical studies of the single SAQDs. Our system provides spatial resolution of $\simeq 0.5\ \mu m$, both in the excitation and the detection channels [14].

The dots position and characteristic emission wavelength are found by taking PL spectra during a line scan over the SAQD sample surface. A typical scan is displayed in Fig. 1, where the PL intensity as a function of photon energy and objective position is given by the gray color scale. During this scan, the PL was excited with a 730 nm, $7\mu W$ cw light from a Ti:S laser. In each 0.1 μm long step of the objective the PL spectrum was measured by exposing a cooled CCD camera for 50 sec. Three emission lines from three different spatial positions along the scanned line are evident in Fig. 1. These lines are due to carriers' recombination within single SAQDs, as indicated by their spatial and spectral widths, which are both resolution limited [6, 17]. In Fig. 2

we present PL spectra from a single SAQD found by such a scan for various excitation powers. An overall perception of the important spectral features is obtained from the 100 μW spectrum which is composed of two groups of emission lines located near 1.325 and 1.375 eV, respectively. The groups are nearly symmetrically positioned around a weak emission line at 1.355 eV. Each group is composed of several sharp and well resolved lines, two of which, roughly 7 meV apart, are particularly strong. We marked the strongest lines in each group and the center line by numbers in increasing order of their spectral position. At excitation power of 1μW, only lines 1 and 3 are observed, at intensity of less than one count per second, in agreement with the estimated exciton lifetime [11] and our system's collection efficiency. The emission of line 1 increases roughly as the square root of the excitation power up to about 100 μW, where it reaches saturation. Line 3, on the other hand, reaches saturation already at excitation power of 7 μW. At 20 μW the emission spectrum is already composed of the five main spectral lines, and at 100 μW, all main lines are saturated. At saturation, the intensity of line 2 is about half that of lines 1, 4 and 5, whose intensity is $\simeq$10 times larger than that of line 3. Above 100 μW, several sharp lines appear below each group of lines. At yet higher excitation power, these lines form two broad spectral bands (C1 and C2, Fig. 2) which dominate the PL spectrum.

For the analysis of our observations we use a model parallelepipedal box with infinite potential barriers and rectangular base whose dimensions are much larger than its height. We fitted the dot base dimensions to obtain the observed level separation of $\simeq$50 meV and adjusted its height to obtain the Coulomb splitting of 7 meV (see below). Using typical InAs effective masses [18] for electrons (0.023 m_0) and for heavy holes (0.6 m_0, where m_0 is the electron rest mass) and dielectric constant [18] ($\varepsilon = 15$) we find that base dimensions of 30.2$\times$31.2 nm^2 and height of 5 nm best fitted the observed data. Note that the box base is not square, thus there is no geometrical degeneracy in agreement with recent calculations[15]. Though our model does not describe the exact SAQD potential structure in geometrical shape [5], strain and piezoelectric fields [16, 15], it is reassuring that the fitted dimensions are similar to those typically reported for this SAQD system [5]. We show below that in spite of its simplicity the model explains our data quite well. This means that the knowledge of the single particle level separation and the strength of the Coulomb matrix elements between these levels are nearly enough to describe the optical properties of a fully quantized system with a few carriers in it. The details of its confining potentials are only second in importance.

We consider the first four, doubly degenerate electron and hole levels in our model dot: (111), (121), (211) and (221) at this energy order, where the numbers in parentheses are the quantum numbers associated with the confinement along the cartesian axes x, y and z (the growth direction), respectively. The wavefunctions of electrons and holes in these states are analytically expressed. This limited number of states is adequate to explain the low level excitation PL spectra. Higher excitation levels, which give rise to carriers in the continuum above the dot barriers' potential, are dealt here more qualitatively. The Coulomb interaction between carriers in our dot is now considered using the following many body Hamiltonian: $H = H_{free} + H_{Coul}$,

where H_{free} describes non interacting electrons (e) and holes (h) in their respective bands, and H_{Coul} describes the e-e, h-h and e-h Coulomb direct and exchange interactions [19]. Since electron and hole wavefunctions are identical in our model, the e-h exchange interaction term vanishes. We find the solution for the multiexciton energy levels and wavefunctions, by exact diagonalization of the the many-body Hamiltonian for these first four single carrier levels. We consider here **all** neutral multi-excitonic states up to exciton population number of eight, at which all the levels considered are fully occupied. Optical transitions between the different excitonic population levels, in which a single e-h pair is annihilated, are then calculated using the dipole approximation [19].

In Fig. 3, horizontal solid lines represent some of the calculated energy levels. The single carrier states (for which the Coulomb interaction is ignored) are displayed on the left side of the figure. Single electron (hole) energy levels are represented by superscripts above the letters e(h) and the occupation number of these levels are given by numbers in front of the letter. The state degeneracy (due to the carriers' spin) is given by the number in parenthesis. The multi-excitonic states, including now the Coulomb interaction between the carriers, are displayed on the right side of the figure. Here, the degeneracy is partially removed and we describe the states by their total angular momentum (S), its projection on the dots growth direction (M_S), and the total electronic (S_e) and hole (S_h) spins. With one exception, indicated by dashed horizontal lines, we display only those states which evolve from single carrier levels of identical electron and hole quantum and occupation numbers. This is because the lowest energy state in each excitonic occupation level is always of this type, and thus, optical transitions between these levels dominate the PL spectrum. These single carrier states are either 1, 4 or 16 times degenerate. The Coulomb interaction lifts only the degeneracy of the 16 multiplets, which occur whenever two half filled levels of electron and hole participate in the multiexcitonic state. They are split into 3 levels according to their S_e and S_h quantum numbers, exactly like a bulk biexciton [20]. The lowest of these levels is 9 fold degenerate containing a quintuplet, a triplet and a singlet of $S_e = 1$ and $S_h = 1$ which add to S= 2,1 and 0, respectively. The mid energy level is 6 fold degenerate containing two triplets of $S_e = 1(0)$ and $S_h = 0(1)$ which add to $S = 1(1)$. The highest of these levels contains only a singlet with $S_e = 0$, $S_h = 0$ and $S = 0$. For calculating the PL spectrum the distribution of excitons among their multi excitonic states should be known. The relatively small number of observed PL lines lead us to safely conclude that only the lowest multi excitonic energy state of each exciton occupation number has a significant steady state population. This means that there is no phonon bottle-neck [21] for exciton thermalization and they reach thermal distribution faster than the radiative recombination occurs.

The optically allowed transitions between the lowest multi excitonic state of each exciton occupation level and the multi excitonic states of one less exciton occupation are represented in Fig. 3 by vertical arrows. Annihilations of e^1h^1 (e^2h^2) are represented by solid (empty) arrows, and annihilation of e^2h^1 is represented by a dash arrow. We note that optical transitions conserve S and M_S [19]. Transitions of the same energy between different exciton occupation levels are drawn along the

same vertical thin dashed line. These vertical lines are numbered in increasing order of their energies, very much like the experimentally measured PL lines as shown in Fig. 4 below. In Fig. 4 we display the calculated dot emission spectra, in units of the squared dipole moment between the e^1 and h^1 states, for a few exciton occupation numbers. In the calculations, we average over degenerate initial states and sum over final states. For comparison, measured spectra for various excitation powers are shown by dots.

The following conclusions are drawn by comparing the experimental data to the model calculations. The characteristic appearance of the PL lines in pairs, is clearly explained in terms of the Coulomb splitting of biexciton levels (the nine and six degenerate levels). The multi line PL spectrum which we measure even at our lowest excitation power, indicates that the average exciton occupation number is already larger than two. This agrees very well with a conservative estimate of the occupation number, based on the measured laser power, and estimations of the absorption and exciton lifetime [11] (Diffusion of carriers from the AlGaAs layers into the SAQD, can be safely neglected due to the sample structure). Thus, surprisingly, single lines due to the recombination of single exciton and single biexciton are not observed at all at low excitation spectra. Line 2, which corresponds in energy to the radiative recombination of a single exciton, appears only at much higher excitation power (20 μW). This can be due to e-h exchange, which splits the four fold degeneracy between the triplet and singlet states of the single exciton level. Since, as has been observed in II-VI nanocrystallites [8], the lower energy triplet state is optically forbidden, the single exciton annihilation line can only be observed when at least three excitons occupy the dot. Alternatively, it can be due to a reduced electron-hole overlap integral which weakens this transition. [15]

Assuming that recombination is possible only via radiative channels we calculated the lifetime of each multi excitonic occupation level. Using these lifetimes in turn, a correlation between the excitation power and the number of excitons within the dots can be drawn. We find a relative good agreement between the excitation power dependence of the PL spectra and the calculated spectra based on that correlation. The appearance of sharp lines at the lower energy side of each of the two spectral line groups, and their evolution with increasing excitation power into the broad bands C1 and C2, are also explained by our model (see the 500 μW PL spectrum in Fig. 4). We note in Fig. 3 that the higher the excitation is, the higher are the populated single electron and hole levels which participate in the multi excitonic ground states. Optical transitions from these states to the high energy states of one less exciton level by the annihilation of e^1h^1 and e^2h^2 are now possible, leading to a characteristic decrease in the energy of these transitions. The magnitude of this shift is given by the Coulomb interaction term between the high energy level and the lower one. This term is almost constant as long as confined single carrier states are concerned. At high enough excitation power, when continuum electron levels are populated, these shifts are becoming smaller and thus, broad spectral bands at low energy are formed. Since the density of continuum levels is large, these bands are not saturated, and they eventually dominate the PL spectra. We do not observe higher energy PL lines due

to the annihilation of higher energy e-h pairs, such as e^3h^3 and e^4h^4 probably since, as can be seen in Fig. 2, they are masked by the large PL emission from the GaAs substrate.

In summary, we resolved the emission from a single self assembled quantum dot and successfully explained its power dependent PL spectra using multi carrier Hamiltonian.

References

[1] M.A. Reed *et al*, Phys. Rev. Lett. **60**, 535 (1988)

[2] K. Brunner *et al*, Phys. Rev. Lett. **69**, 3216 (1992); **ibid**, **73**, 1138 (1994)

[3] C.W. Sneyder *et al*, Phys. Rev. Lett. **66**, 3032 (1991)

[4] J.-Y. Marzin *et al*, Phys. Rev. Lett. **73**, 716 (1994)

[5] H. Drexler *et al*, Phys. Rev. Lett. **73**, 2252 (1994)

[6] D. Gammon *et al*, Phys. Rev. Lett. **76**, 3005 (1996)

[7] U. Bockelmann *et al*, Phys. Rev. Lett. **76**, 3622 (1996)

[8] M. Nirmal *et al*, Phys. Rev. Lett. **75**, 3728 (1995)

[9] W. Wegscheider *et al*, Phys. Rev. Lett. **79**, 1917 (1997)

[10] S. Fafard *et al*, Phys. Rev. **B 52**, 5752 (1995)

[11] S. Raymond *et al*, Phys. Rev. **B 54**, 11548 (1996)

[12] M. Grundmann *et al*, Phys. Rev. Lett. **74**, 4043 (1995)

[13] V.A. Shchukin *et al*, Phys. Rev. Lett. **75**, 2968 (1995)

[14] E. Dekel *et al*, Physica E (in press).

[15] J. Kim *et al*, Phys. Rev. **B 98**, (in press).

[16] C. Pryor *et al*, Phys. Rev. **B 56**, 10404 (1997)

[17] H.F. Hess *et al*, Science **264** , 1740 (1994)

[18] S. Adachi J. Appl. Phys. **58**, R1, (1985)

[19] A. Barenco and M.A. Dupertuis, Phys. Rev. **B 52**, 2766 (1995)

[20] J.J. Forney *et al*, Nuovo Cimento B **22**, 153 (1974)

[21] H. Benisty, Phys. Rev. **B 51**, 13281 (1995)

Figure Captions

Fig. 1 PL intensity as a function of photon energy and position along a line across the SAQD sample surface. The intensity is given by color scale bar to the right. Left inset: schematic description of the sample. Right inset: far-field PL spectrum of the sample.

Fig. 2 PL spectra from a single SAQD for various excitation power levels.

Fig. 3 Energy level diagram of the SAQD multiexcitonic states, contributing the most to optical emission. Shown are the multiexcitonic levels calculated by excluding (left) and including (right) the Coulomb interaction between carriers. The vertical arrows indicate optical transitions due to one exciton annihilation, (see text).

Fig. 4 Calculated PL spectra for various exciton population numbers. For comparison, the experimental measurements are also displayed.

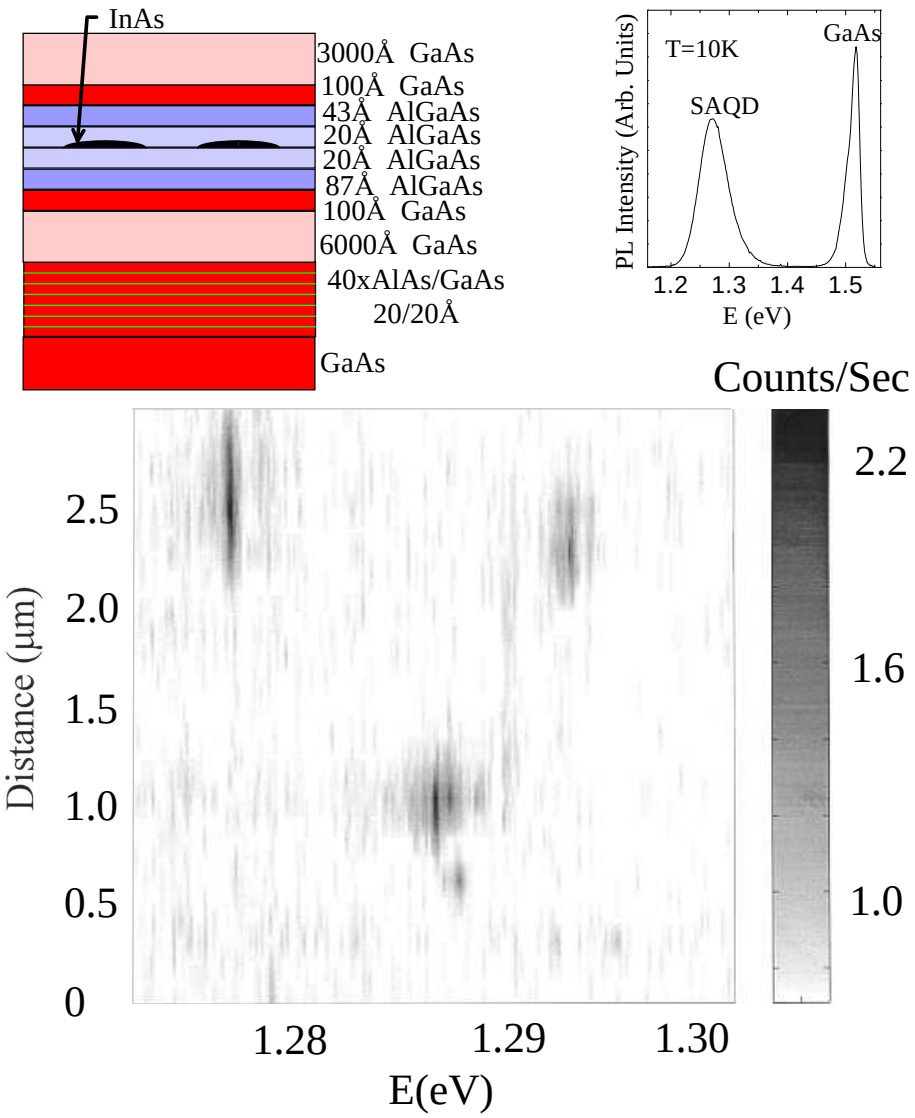
InAs
3000Å GaAs
100Å GaAs
43Å AlGaAs
20Å AlGaAs
20Å AlGaAs
87Å AlGaAs
100Å GaAs
6000Å GaAs
40xAlAs/GaAs
20/20Å
GaAs
T=10K
SAQD
GaAs
PL Intensity (Arb. Units)
1.2
1.3
1.4
1.5
E (eV)
Counts/Sec
2.2
1.6
1.0
Distance (μm)
2.5
2.0
1.5
1.0
0.5
0
1.28
1.29
1.30
E(eV)

Fig.1

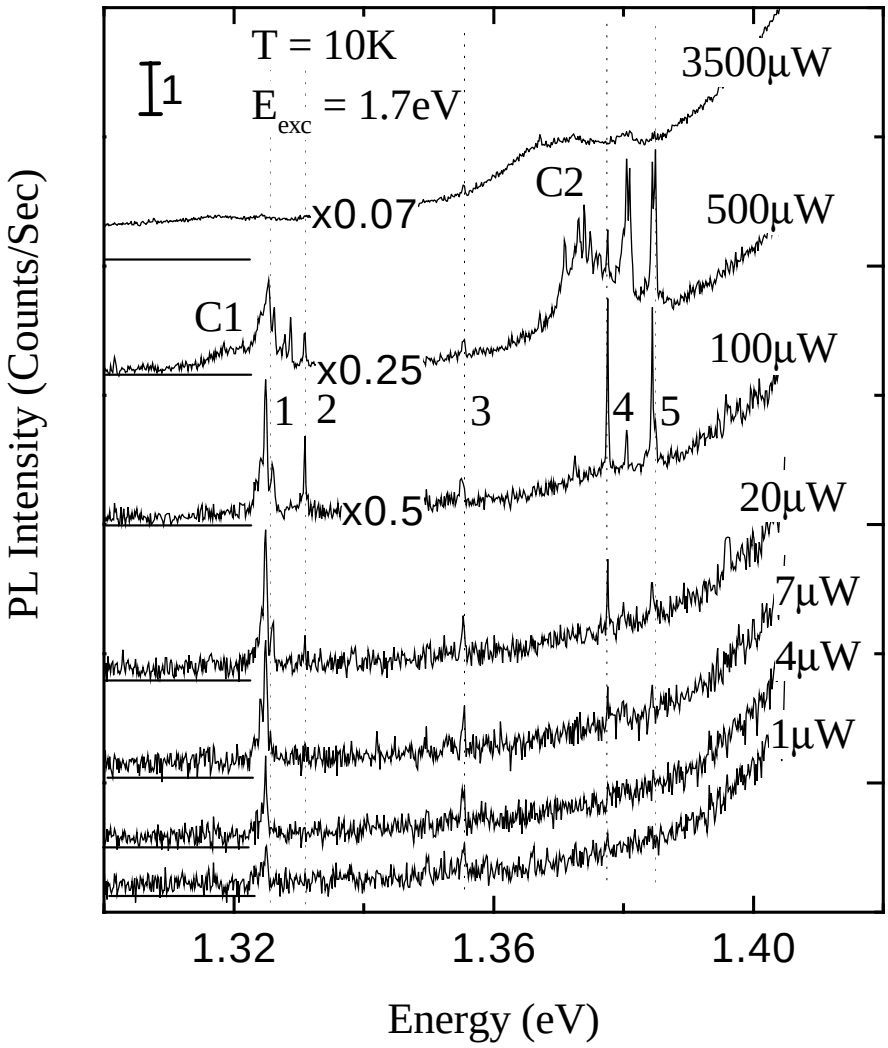
T = 10K
E_exc = 1.7eV
1
3500μW
x0.07
C2
500μW
C1
x0.25
100μW
1
2
3
4
5
x0.5
20μW
7μW
4μW
1μW
1.32
1.36
1.40
Energy (eV)
PL Intensity (Counts/Sec)

Fig.2

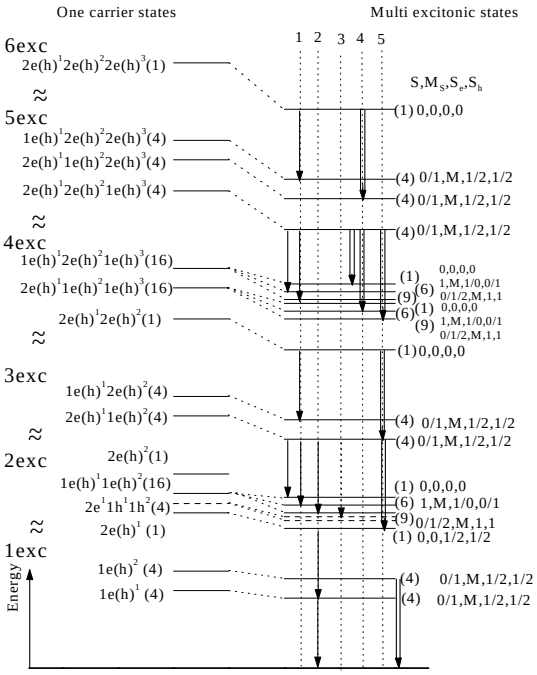
One carrier states
Multi excitonic states
1 2 3 4 5
6exc
2e(h)1 2e(h)2 2e(h)3 (1)
5exc
1e(h)1 2e(h)2 2e(h)3 (4)
2e(h)1 1e(h)2 2e(h)3 (4)
2e(h)1 2e(h)2 1e(h)3 (4)
4exc
1e(h)1 2e(h)2 1e(h)3 (16)
2e(h)1 1e(h)2 1e(h)3 (16)
2e(h)1 2e(h)2 (1)
3exc
1e(h)1 2e(h)2 (4)
2e(h)1 1e(h)2 (4)
2exc
2e(h)2 (1)
1e(h)1 1e(h)2 (16)
2e1 1h1 1h2 (4)
2e(h)1 (1)
1exc
1e(h)2 (4)
1e(h)1 (4)
Energy
S,Ms,Se,Sh
(1) 0,0,0,0
(4) 0/1,M,1/2,1/2
(4) 0/1,M,1/2,1/2
(4) 0/1,M,1/2,1/2
(1) 0,0,0,0
(6) 1,M,1/0,0/1
(9) 0/1/2,M,1,1
(1) 0,0,0,0
(6) 1,M,1/0,0/1
(9) 0/1/2,M,1,1
(1) 0,0,0,0
(4) 0/1,M,1/2,1/2
(4) 0/1,M,1/2,1/2
(1) 0,0,0,0
(6) 1,M,1/0,0/1
(9) 0/1/2,M,1,1
(1) 0,0,1/2,1/2
(4) 0/1,M,1/2,1/2
(4) 0/1,M,1/2,1/2

Fig.3

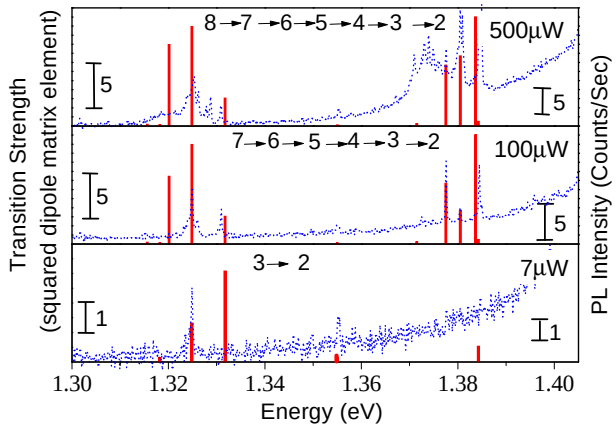
Transition Strength
(squared dipole matrix element)
8→7→6→5→4→3→2
500μW
5
5
7→6→5→4→3→2
100μW
5
5
3→2
7μW
1
1
PL Intensity (Counts/Sec)
1.30
1.32
1.34
1.36
1.38
1.40
Energy (eV)

Fig.4